JOURNAL OF PROPULSION AND POWER
Vol. 23, No. 3, May–June 2007

Ground Chamber Measurements of the Electromagnetic Emissions from the Hayabusa Ion Engine

Kazutaka Nishiyama,* Yukio Shimizu,† Ikkoh Funaki,* and Hitoshi Kuninaka‡
Japan Aerospace Exploration Agency, Kanagawa 229-8510, Japan
and
Kyoichiro Toki§
Tokyo University of Agriculture and Technology, Tokyo 184-8588, Japan

DOI: 10.2514/1.19473

Radiated electric field emissions from the prototype model of the ion engine system of the asteroid explorer Hayabusa (MUSES-C) were measured in approximate accordance to MIL-STD-461C. The typical noise level exceeded the narrowband specification at frequencies less than 5 MHz. The microwave discharge neutralizer generates broadband noise and narrowband oscillations that have a fundamental frequency of about 160 kHz and are accompanied by its harmonics up to the fifth. Leakage of 4.25 GHz microwaves for plasma production and its second harmonic were 65 dB and 35 dB above specifications, respectively. The X-band receiver onboard Hayabusa measured the noise from the ion engine system at the uplink frequency of 7.16 GHz through a horn antenna. This susceptibility test showed that the microwave discharge ion thruster is unlikely to interfere with deep space microwave communication.

Nomenclature

d = neutralizer orifice diameter
I_D = electron emission current of the neutralizer
l = anode distance from the neutralizer
$\dot{m}$ = xenon flow rate
P_μ = microwave power for plasma discharge of the neutralizer
V_D = voltage between the neutralizer and the anode in diode mode operation

I. Introduction

IN SATELLITES driven by electric propulsion, a considerable amount of electric power generated in space is put into discharge plasma. Many cases exist in which exposing the current path to space is inevitable, thereby creating a large electromagnetic noise source. A review by Sovey et al. [1] describes results of ground-based and flight tests of electromagnetic interference (EMI) in electric propulsion systems that date back to the 1980s. As for ion propulsion systems developed after the SERT-I project, which is considered to be the first ion thruster flight, all of them including the Japanese ETS-III [2,3], ETS-VI [4], German RIT-10 [5], and British T5 [6] have undergone ground-based EMI tests. It is usual practice to follow the U.S. military standard MIL-STD-461 for EMI documentation of components onboard satellites, but such requirements have not been fully satisfied by any electric propulsion systems (whether they be ion thrusters or other type) developed up until now. In the case of NASA's NSTAR ion engine used by the DS1 probe, which is presently operating in interplanetary space, an EMI measuring device (Plasma Wave Detector) is onboard as one of several environment-measuring devices [7].

An ion engine system (IES) for the MUSES-C asteroid sample return mission was developed at the Institute of Space and Astronautical Science (ISAS), Japan [8]. The spacecraft, named Hayabusa, was launched on 9 May 2003 on an ISAS M-V rocket from the Kagoshima Space Center located on the southern tip of the Japanese island of Kyushu. Hayabusa's EMI specifications, which are applied to all onboard components, are a modification of the radiated emission (RE) specification of MIL-STD-461C (RE02). The Hayabusa/IES is the first ion propulsion system using microwave discharges; its electromagnetic compatibility (EMC) with spacecraft was a concern. Although it was estimated that microwaves of 4.25 GHz generated by traveling wave tube amplifiers could leak to some extent, what sort of electromagnetic noise is radiated and the exact location were questions that remained to be answered. Accordingly, we conducted two RE02 measurements: one involving both an ion engine μ10 and a neutralizer, and another one solely for the neutralizer.

Degradation of the sensitivity of the X-band receiver (XRX) is caused when the radiated emission from IES is greater than the thermal noise level in the uplink frequency of the Hayabusa's XRX. In the RE specification of the Hayabusa deep space probe, spurious radiations in the frequency range of ± 5 MHz with centers of 7.16 and 6.36 GHz are limited, respectively, to -6, $+34$ dB $\mu\mathrm{V}\cdot\mathrm{m}^{-1}$. The former is for the XRX signal band and the latter is for its image band. Only these two were modified from the narrowband RE02 specification of the MIL-STD-461C. It is difficult to measure such weak noise using standard EMI test equipment. Therefore, a compatibility test using IES and XRX was necessary to ensure that the IES satisfied the requirements. Hence, an interference check that used a radio frequency/intermediate frequency (RF/IF) signal processing part of the XRX as a high-gain amplifier was carried out after the IES' EMI test. A general concern exists about the attenuation and phase change of the communication wave propagated through the plasma plume. Although this is also one type of EMC problem between the electric propulsion and the communication systems of the satellite, we consider this not to be the case for Hayabusa, in which thruster plume density is too low to degrade the communication link, according to results of experiments and analyses [9].

Received 14 August 2005; revision received 19 June 2006; accepted for publication 11 December 2006.

*Associate Professor, Institute of Space and Astronautical Science, 3-1-1 Yoshinodai, Sagamihara. Member AIAA.
†Engineer, Institute of Space and Astronautical Science, 3-1-1 Yoshinodai, Sagamihara. Member AIAA.
‡Professor, Institute of Space and Astronautical Science, 3-1-1 Yoshinodai, Sagamihara. Member AIAA.
§Professor, Graduate School of Bio-Applications and Systems Engineering, 2-24-16 Naka-cho, Koganei. Member AIAA.

Table 1 Summary of Hayabusa/IES EMI tests

	IES RE02 & X-band receiver interference		Neutralizer RE02	IES CE
Environment	Anechoic chamber		EMI chamber	IES endurance test room
Chamber	Upright cylindrical glass chamber		T-shaped glass chamber	Metal chamber
Pumping system	1 cryogenic pump		1 oil diffusion pump and 1 rotary pump	8 cryogenic pumps
Vacuum pressure and xenon flow rate	1.1×10^{-3} Pa@2.25 SCCM		7×10^{-3} Pa@0.5 SCCM	1.5×10^{-4} Pa@3 SCCM
μ10 ion source	PM		——	PM
Neutralizer	PM		PM	PM
PPU	GSE		GSE	GSE/IPPU (PM)
Microwave generator	FM		GSE	GSE
Propellant feed system	GSE		GSE	GSE
Thruster controller	ITCU (PM)		Personal computer	Workstation
Frequency	14 kHz − 10 GHz, 7.16 GHz		14 kHz − 1 GHz	0 Hz–50 MHz
Spectrum analyzer, preselector, and preamplifier	HP8566B + HP85685A + HP8459B			HP856E
Detector mode	Quasi peak			Positive peak
	Antenna types and 3 dB resolution bandwidths for RE measurements			3 dB resolution bandwidths for CE measurements
Frequency range	Narrowband	Broadband	Antenna	3 kHz (0–300 kHz)
14–100 kHz	300 Hz	1 kHz	Active monopole type EMCO 3301B	10 kHz (0–1 MHz)
100 kHz–30 MHz	1 kHz	3 kHz	Active monopole type EMCO 3301B	30 kHz (0–5 MHz)
30–200 MHz	3 kHz	10 kHz	Biconical type EATON 94455-1	300 kHz (0–50 MHz)
200 MHz–1 GHz	10 kHz	30 kHz	Log spiral type EATON 93490-1	Current probe
1 GHz–10 GHz	30 kHz	100 kHz	Log spiral type EATON 93491-2	Tektronix, Inc. P6021 probe and model 134 amplifier
Video bandwidth	10 times larger than the resolution bandwidth	10 times larger than the resolution bandwidth		Equals the resolution bandwidth

In addition to radiated emissions, conducted emissions (CE) from the IES power processing unit (IPPU), for the ion beam acceleration with a power consumption of 1.2 kW and with three thruster units operating via the spacecraft power bus line were also investigated. The CE specification of Hayabusa differs from the CE01/03 of MIL-STD-461C. Although the frequency range of the Hayabusa specification is 30 Hz–50 MHz, which is the same as that defined in CE01/03, the emission limit is relaxed at frequencies higher than 10 kHz by 20 dB at most; it is stricter at frequencies lower than 10 kHz by 20 dB at most. The CE measurement of the noise in the power line current was conducted using a prototype model (PM) of the IPPU and a commercial power supply as an unstabilized power bus simulator. Measurements of conducted noise on the screen grid line and neutralizer line from IPPU were also carried out to examine correlation with the conducted noise on the bus line, as well as the noise source.

II. Experimental Arrangement

This paper reports three EMI test results, which are summarized in Table 1. The measurement receiver bandwidths listed in this table were used for emission testing. These bandwidths are specified at the 3 dB down points for the overall selectivity curve of the receivers. Video bandwidth was controlled so that it was set to a 10 times greater value than the spectrum analyzer resolution bandwidth. The Hayabusa RE spec has separate narrowband and broadband limits as in MIL-STD-461C. Therefore, both narrowband and broadband E-field emissions were measured sequentially before antenna switching. All measurements were carried out using a spectrum analyzer with a quasipeak detector. In RE02 measurements, several types of antennas, which were selected depending on the frequency range, were used as well as a preamplifier, a preselector, and a spectrum analyzer. These antennas include an active monopole, a biconical one, and two conical log spiral antennas of different sizes depending on the frequency range. Horn antennas, spectrum analyzers, and a digital voltmeter were employed in interference tests with the XRX. Antenna factors, cable losses, and preamp gains were all calibrated and input to the EMI test software as a function of frequency in advance. In several experimental setups, for glass chamber wall protection from contamination by sputtered metallic atoms that degrade the transmittance of electromagnetic emissions, the glass inner surface was covered with a polyethylene terephthalate (PET) film, which was replaced after every 30 min of thruster operation. Because the transmittance of electromagnetic waves of glasses and PET films had not been well controlled and calibrated, this is one source of experimental uncertainty.

The entire engine subsystem and single neutralizer were operated in two modes: the "beam mode" and the "discharge mode." In the beam mode, voltages were applied to both the ion source (1500 V) and the neutralizer (about −30 V relative to the spacecraft potential), and ion beam and electrons were extracted, respectively. In the discharge mode, microwave was applied to generate the chamber plasma and the neutralizer plasma, but no currents were extracted because both plasma sources were set at ground potential.

A. Radiated Emission from the IES and Interference with the X-Band Receiver

The $20 \times 8.6 \times 8.6$ m anechoic chamber and the measurement room at ISAS are shown schematically in Fig. 1. This facility has radio wave absorbers attached to all wall surfaces, as well as to the ceiling and the floor, with electromagnetic shields. The 1.0 m high pyramid type wave absorbers made of carbon graphite-impregnated urethane foam provide absorption of < -30 dB (30–200 MHz) and −40 dB above 500 MHz at normal incidence. The copper-plated steel walls provide >60 dB shielding from 30 kHz–30 GHz. This chamber is used for antenna pattern measurements, EMC tests between observation equipment and telemeters or radar transponders of either scientific satellites or rockets, and for tests involving observation equipment with wireless transmission functions. In the

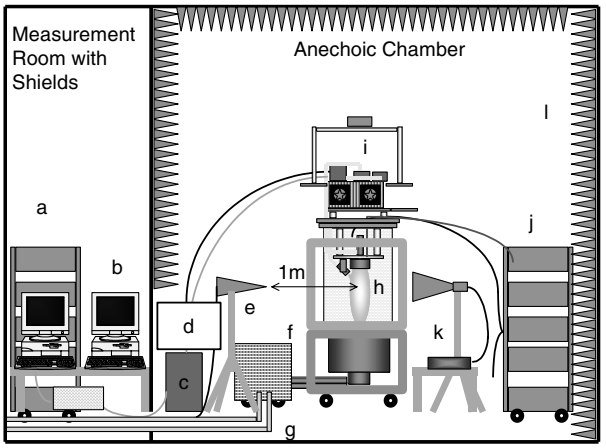

Fig. 1 Experimental setup to measure radiated emissions from Hayabusa/IES and to check interference with the X-band receiver: a) EMI measurement system, b) PCs for command and telemetry of the ion engine subsystem, c) ITCU, d) spacecraft 50 V bus simulator, e) antennas for RE02 measurements, f) cryopump with helium compressor, g) cooling water, h) ion thruster with neutralizer inside glass chamber, i) microwave supply unit with cooling fan and clean booth, j) dc power supplies and xenon feed system, k) an X-band receiver and double ridge horn antenna, and l) pyramid wave absorbers.

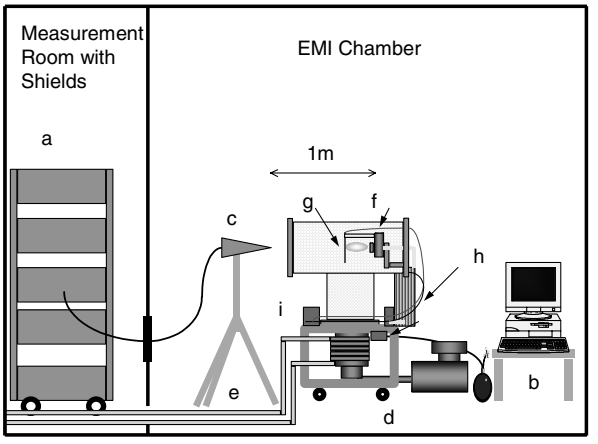

Fig. 2 Experimental setup to measure radiated emissions from the neutralizer: a) EMI measurement system, b) PC for neutralizer control, c) antennas for RE02 measurements, d) oil diffusion and rotary pumps, e) cooling water, f) neutralizer inside a T-shaped glass chamber, g) anode, h) solid-state microwave amplifier, and i) dc power supplies and xenon feed system.

RE02 measurement and XRX interference test, a PM of the IES thruster control unit (ITCU), a PM of microwave oscillator,and a flight model (FM) of a traveling wave tube amplifier (TWTA), a PM of μ10 ion source, and a PM of neutralizer were used. However, a PM of an IPPU, which was not available because of its tight schedule, and propellant feed system that was considered low risk for EMI emission were replaced with ground support equipment (GSE) comprising a mass flow controller and commercial high-voltage DC power supplies.

Radiated emissions from the IES can be classified into two categories: 1) emission having its origin at the IPPU, such as switching noise or ripples; 2) noise emanating from the plasma acting as a "load," which appears when the IPPU is operated in combination with the ion source and the neutralizer. The former can be reproduced easily and tackled through tests using resistive loads simulating ion thruster heads. No difference existed in conducted noise emission on the screen- and decel-grid lines between the case using a GSE and the case using an IPPU, except apparent switching noises of IPPU at the switching frequency and its harmonics. Therefore, if we concentrate on the noise originated from the plasma, the RE measurement result in the GSE operation can be considered same as the measurement result of IES with the EMI optimized flight model of the IPPU.

It is difficult to measure electromagnetic emissions from the ion engine system because of the metallic tank that is necessary for its usual operation on the ground. Therefore, a glass chamber consisting of a cryopump, a cylindrical glass wall, and an IES-mounting metal flange was prepared. An ion thruster and a neutralizer hang from the top flange, and the chamber was evacuated using the cryopump. The IES was operated at Xe flow rates of 1.85 standard cubic centimeters per minute (SCCM) for the main discharge and 0.4 SCCM for the neutralizer, which correspond to 80% of the nominal thrust level, because of the limited exhaust capability of the cryopump. With this lower flow rate, the higher background pressure in the glass chamber increased the ion beam current to over 130 mA, which corresponds to the nominal thrust level of 7 mN.

B. Radiated Emission from the Neutralizer

The experimental setup to measure radiated emissions from the neutralizer is shown in Fig. 2. Electromagnetic shielding of the $5.4 \times 5.5 \times 3.5$ m EMI chamber at ISAS is greater than 105 dB from 30 kHz–30 GHz; it is much better than the anechoic chamber described before, and EMI measurements of small onboard equipment are usually conducted in this room. The cylinder glass chamber was too large to be carried in the EMI chamber. Therefore, it was not possible to carry out IES radiation noise measurement here. A 30 mm^2 punching steel plate, acting effectively as an anode, was placed 20 mm downstream from the neutralizer. As a microwave supply system, a GSE that consisted of an oscillator and a solid-state amplifier was used. The neutralizer was installed in the small T-shaped glass chamber, evacuated with an oil diffusion pump, and an electron current equivalent to that of nominal IES operation was extracted.

C. Conducted Emission from the IES

This measurement was performed in a room with ion engine endurance testing capabilities, which was not shielded from external electromagnetic noise. The measurement of the conducted noise can be carried out simply by installing current probes for wirings; effects of external noise were not observed whatsoever. Although the wirings used were common vinyl lines and were not flight-qualified, this had no effect on the measurement results, even if they had been replaced with well-shielded coaxial cables. Accordingly, the cable type was considered to be independent of the properties of the conducted noise. Measurements were carried out at three points: the screen-current line, neutralizer-current line, and hot line of the spacecraft bus simulator. The bus simulator was a regulated dc power supply used as a replacement of solar array paddle of the spacecraft. The voltage was changed 70–110 V to investigate the IPPU characteristics to the bus voltage. No 10 μF capacitors or line impedance stabilization networks or metallic ground plane, which are defined as requirements in MIL-STD-462, were used. Therefore, these tests were not compliant with CE01/03 of MIL-STD-461C. Because the PM of the IPPU had not been well tuned considering the EMI characteristics at that time and had its own switching noise independent of the load characteristics, measurements were also carried out with the IES operating with a GSE to distinguish plasma-oriented noise.

III. Experimental Results and Discussion

A. RE02 Background Noise

Concerning radiated emission measurements, in approximate accordance to RE02 specification of MIL-STD-461C, background noise was observed at the onset of the experiment, when the ITCU and GSE including a computer, vacuum pumps, and dc power supplies were all kept switched on, but were not in operation. Figures 3a and 3c show much more noise in the anechoic chamber than in the EMI chamber at frequencies less than 1 GHz because of the superior electromagnetic shielding capability of the EMI chamber. In the anechoic chamber, the external noise was more remarkable than the noise generated by the equipment inside. In both

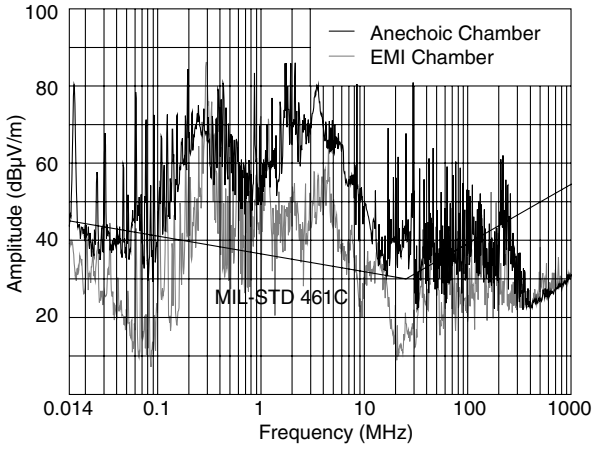

a) Narrowband 14 kHz–1 GHz

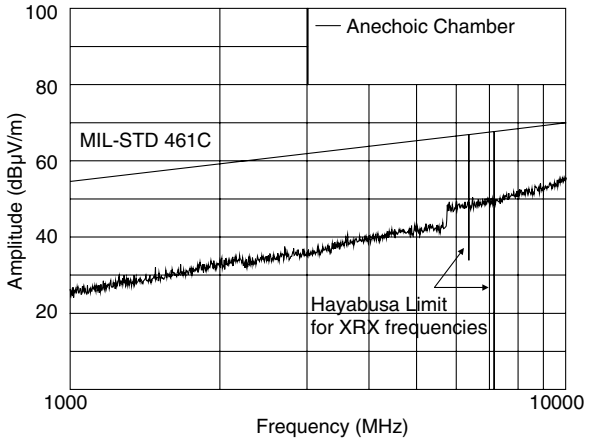

b) Narrowband 1–10 GHz

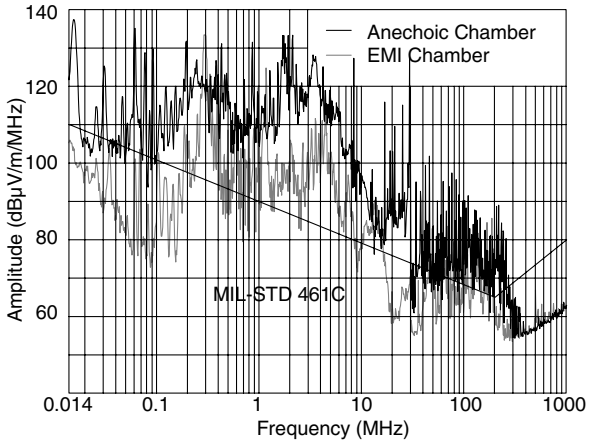

c) Broadband 14 kHz–1 GHz

Fig. 3 RE02 background noise and EMI specification of Hayabusa spacecraft.

facilities there were many frequency bands in which background noise deviated from the restriction of MIL-STD shown by the polygonal line in Fig. 3a for narrowband and Fig. 3c for broadband, respectively. They are not ideal for noise measurement. However, good shielding characteristics were shown for frequencies over ultrahigh frequency (UHF), which are often used for telecommunications. In them, no noise exceeded the internal noise of measuring instruments over 1 GHz. Only the narrowband result of the anechoic chamber is shown in Fig. 3b. The straight line, which shows a monotonous increase in Fig. 3b, provides the MIL-STD-461C specification. The two added notches indicate an uplink frequency of 7.16 GHz for Hayabusa's XRX and its image frequency of 6.36 GHz.

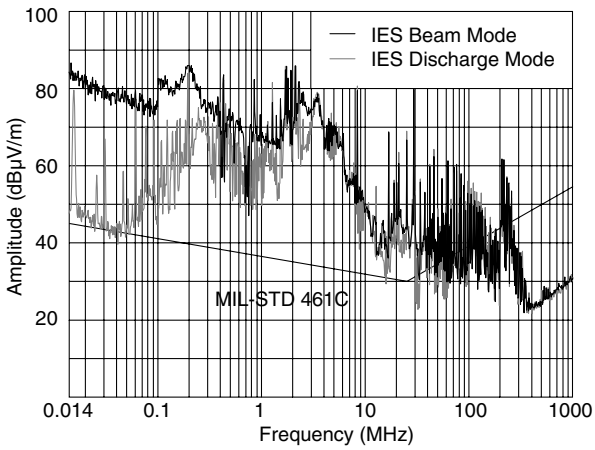

a) Narrowband

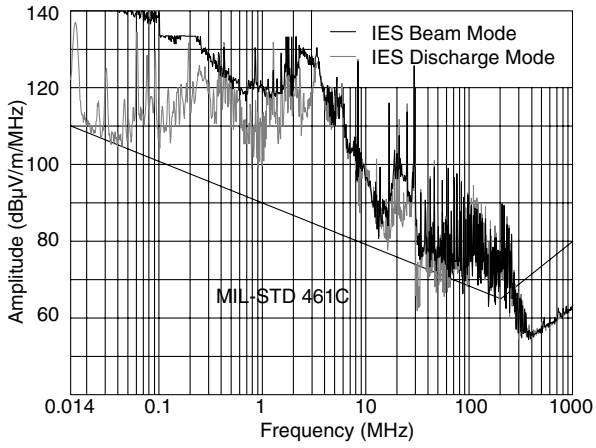

b) Broadband

Fig. 4 RE02 noise from the ion engine system in discharge mode and in beam mode; 14 kHz–1 GHz.

B. RE02 14 kHz–1 GHz

Low-frequency noise spectra under 1 GHz during IES operation are shown in Fig. 4 for both narrowband and broadband emissions. Lower traces of Figs. 4a and 4b portray noise emissions of plasma discharge mode from the ion source and the neutralizer. No IES emissions larger than the background noise existed in the anechoic chamber, as shown in Fig. 3. Once the high-voltage dc power supply was turned on and the ion beam acceleration was started, a broadband noise with a tendency for the intensity to increase at lower frequencies, and which is apparently larger than background noise as shown in Fig. 4, was generated. This exceeds the restriction by 30–40 dB at frequencies under 5 MHz. Even though several sharp upsurges and drops exist in the 2–4 MHz frequency range, it remains unclear whether this is caused by the IES operation because the background noise reaches its maximum level around these frequencies; its random fluctuation might influence the result. It is noteworthy that broadband emissions in the beam mode exceeded the receiver saturation level at frequencies around 200 kHz and <40 kHz for the broadband sweep.

Figure 5 shows results of the neutralizer operations in the EMI chamber. This set of data shows smaller effects of background noise. It remains unclear why emissions by the neutralizer discharge by itself, as shown in Fig. 5, are at most 20 dB larger than the emission by both main and neutralizer discharges, as shown in Fig. 4. Upper traces of Fig. 5 show the noise when the electron current is extracted to the anode from the neutralizer at a bias voltage of about 30 V. This noise spectrum resembles the spectrum emitted by the IES during beam acceleration, as shown in Fig. 4b, indicating that most of the low-frequency noise of less than 5 MHz originates from the neutralizer plasma. Similar results for neutralizer noise have also been reported for the T5 ion thruster [6] in combination with a

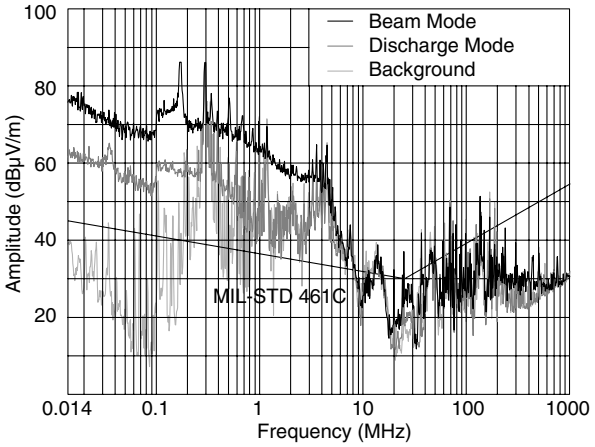

a) Narrowband

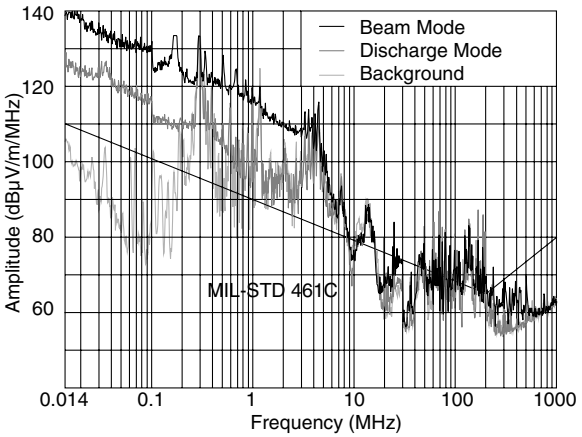

b) Broadband

Fig. 5 RE02 noise from the neutralizer in discharge mode and in beam mode; 14 kHz–1 GHz.

Kaufman-type ion source and a hollow cathode neutralizer. It will be added that both devices adopted a plasma production mechanism that is completely different from the one in the Hayabusa/IES'.

C. CE 100 kHz–30 MHz for Power Line and Noise in Screen and Neutralizer-Current Lines

Measurements of conducted emissions on the IPPU input lines from the spacecraft bus were intended to verify that thruster and/or IPPU generated noise conducted back to the bus via this path are within limits to protect other items also on the bus. IPPU input and output filters help reduce such CE. Hayabusa mission does not require measurements of CE between the IPPU and thruster heads. However, such measurements on IES interconnect wires do help in identifying the source of CE and in evaluating the effectiveness of IPPU filters. Thus, in addition to the standard CE measurements on IPPU input power line, conducted emissions were also monitored on IES interconnect lines including current-to-screen grid and neutralizer. The neutralizer and the decelerator grid were wired at the same potential in such IES.

Figures 6–8 show spectra of the conducted noise on screen current and neutralizer current in the case of using the GSE of dc power supplies instead of an IPPU. The units shown on the vertical axes of the graphs for the CE results are given in dB μA. Its maximum value of 113 dB μA corresponds to a current amplitude of 447 mArms (the root mean square value of the current). Figures 6 and 7 show the change of low-frequency noises of less than 300 kHz that were measured in the screen-current line and the neutralizer-current line in plasma discharge mode and in beam acceleration mode. The noise of the neutralizer current is much larger than that of the screen current in beam acceleration mode, although the noises in plasma discharge mode are small for both. This fact is readily apparent merely by

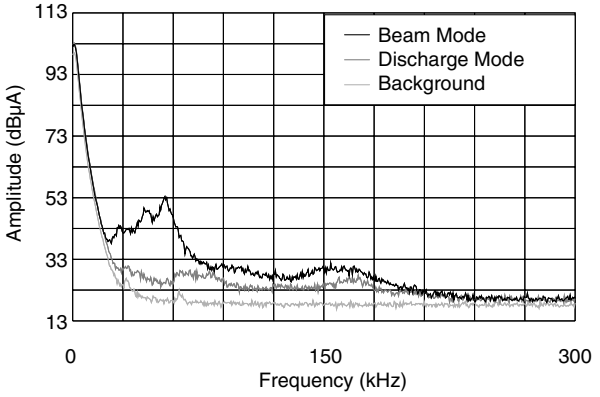

Fig. 6 CE measurement result for screen grid line over the frequency range 0–300 kHz.

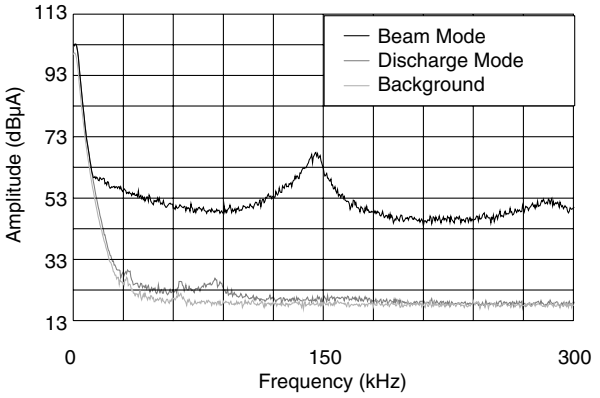

Fig. 7 CE measurement result for the neutralizer line over the frequency range 0–300 kHz.

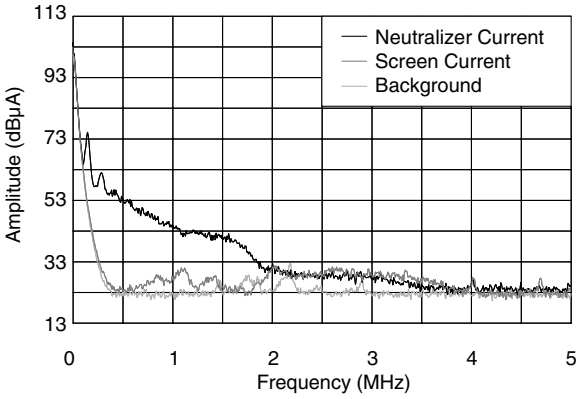

Fig. 8 CE measurement results for screen grid line and neutralizer line over the frequency range 0–5 MHz.

monitoring neutralizer-current history with a multichannel digital recorder that a 5-Hz filter function should be enabled to eliminate the noise whose amplitude reaches 70% of the neutralizer current. On the neutralizer line, coherent oscillations with a fundamental frequency of 160 kHz and its harmonics up to the fifth were observed.

Conditions of oscillation generation and the characteristic frequency are dependent on xenon flow rates and neutralizer currents. Oscillation was observed not only in the conducted noise on the neutralizer line shown in Fig. 7, but also in radiated emission spectra measured by operating the neutralizer by itself, as shown in Fig. 5b. Although the narrowband noise peak found in the radiated emission from the IES shown in Fig. 4b has a slightly higher frequency of about 200 kHz, it might be regarded fundamentally as the same phenomenon. The oscillation reappeared at the same frequency along with additional switching noise from the IPPU at other frequencies when an IPPU instead of GSEs was used; it was

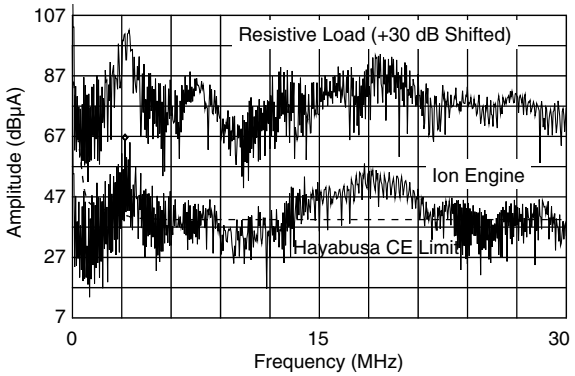

Fig. 9 CE measurement result for IPPU's power line over the frequency range of 100 kHz–30 MHz, compared with the result in resistive load operation.

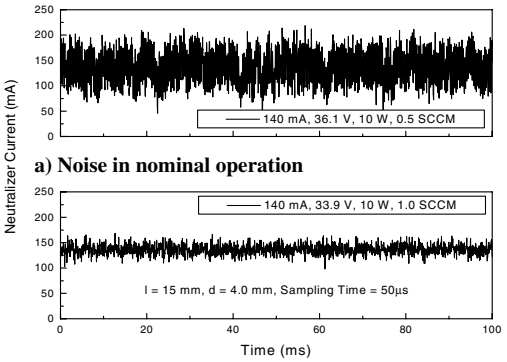

a) Noise in nominal operation

b) Less noise at a larger mass flow rate

Fig. 10 Time domain waveforms of the neutralizer current.

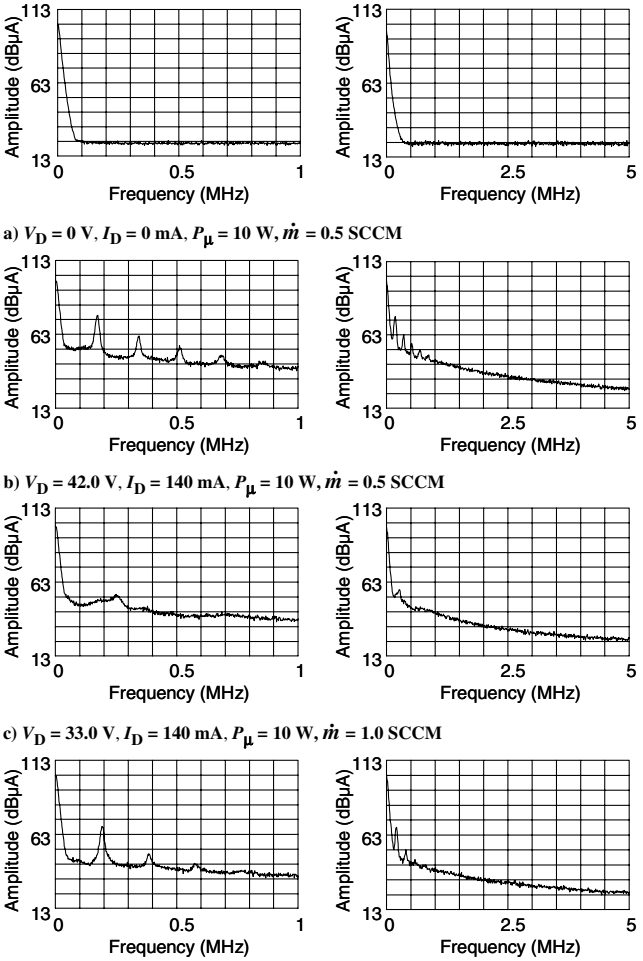

a) V_D = 0 V, I_D = 0 mA, P_μ = 10 W, $\dot{m}$ = 0.5 SCCM

b) V_D = 42.0 V, I_D = 140 mA, P_μ = 10 W, $\dot{m}$ = 0.5 SCCM

c) V_D = 33.0 V, I_D = 140 mA, P_μ = 10 W, $\dot{m}$ = 1.0 SCCM

d) V_D = 62.1 V, I_D = 140 mA, P_μ = 5 W, $\dot{m}$ = 0.5 SCCM

Fig. 11 Noise spectra of neutralizer current. $l = 20$ mm, $d = 4.5$ mm, 10 dB/div.

also the case when the operation of only the neutralizer was performed. This equivalence implies that the neutralization processes in the ion beam and the power supply characteristics are unrelated to both the oscillation and the low-frequency noise. Results concerning a more detailed investigation of the correlation between neutralizer operating conditions and the oscillation, as well as its generation mechanism, will be reported later in this paper.

The noise tails of the screen current and neutralizer at high frequencies up to 5 MHz are both shown in Fig. 8. As for the neutralizer, there is almost no noise over 4 MHz. Figure 8 shows that the screen current contains a small amount of noise in the 500 kHz–4 MHz frequency range. Incidentally, this finding cannot be estimated merely by inspecting Fig. 6, which shows the decrease at relatively higher frequencies immediately below 300 kHz.

Although there was conducted noise correlative with radiated noise in the wires connected with the ion thruster head, noise caused by the engine was not observed in results concerning CE measurements of the simulated spacecraft power line to the IPPU, as shown in the lower data of Fig. 9. The upper trace of Fig. 9 shows the result when operating the IPPU connected to resistors as dummy loads replacing the thruster head. However, significant differences were not found in those results, even in the low-frequency region where the RE and CE appear. This is probably because most of the power consumption by the IPPU is made by the beam current with much less noise, and the noise power of the neutralizer is too small to influence the bus power. By raising the frequency resolution of the spectrum analyzer, it turned out that the power line current noise consists of switching noise of the IPPU at frequencies of 100 kHz and its very high-order harmonic components. However, at present, irrespective of whether a resistive or plasma load is considered, the noise level exceeds the Hayabusa specification limits, which require emissions lower than 40 dB μA above 4 MHz. It was judged that elimination of the switching noise leak will be easy when manufacturing the FM of the IPPU because circuit design and mounting considering the EMI characteristics had not been completely carried out in the PM of the IPPU. The test clarified the fact that the noise from IES plasma does not affect the spacecraft power bus. Therefore, the EMC tuning of the flight model was conducted with the IPPU by itself without fitting to other IES components.

D. More Details on the Low-Frequency Neutralizer Noise

To understand characteristics of noise emission from the neutralizer at low frequencies, further parametric studies were carried out using only the neutralizer without the ion source as shown in Fig. 2. Figure 10 shows two typical time histories of the neutralizer current recorded with a digital memory recorder at the relatively slow sampling time of 50 μs. At a xenon flow rate of 0.5 SCCM, noise with an amplitude as large as the 140 mA direct current component was detected, as shown in Fig. 10a. Nonetheless, it decreased in overall amplitude to 1/3 of the noise level shown in the upper trace, at an excessive flow rate of 1.0 SCCM, as shown in Fig. 10b.

Frequency spectra of the conducted neutralizer noise are shown in Fig. 11 for several operating conditions. Broadband noise below 5 MHz and narrowband noise by coherent self-oscillation can be seen with harmonics. In the case with just a plasma discharge without electron extraction taking place, conducted emissions were not observed, as shown in Fig. 11a. If the neutralizer electron current was gradually increased from 0 to 140 mA, the broadband noise was found to grow at larger electron currents of 15 mA then saturate over 70 mA. Comparison of Figs. 11b and 11c shows that increasing xenon flow decreases broadband noise and suppresses oscillation. Comparison of Figs. 11b–11d suggests that the broadband noise and the coherent oscillation are reduced by decreasing the microwave

Table 2 Coherent oscillation occurrence probability and parameters relating to the shape of plasma plume

d/l, mm	10	15	20	30
4.0	b	a	a	a
4.5	c	a	a	a
5.0	d	b	a	a
5.5	d	d	c	a
6.0	d	d	d	b

[a]Oscillation observed at various currents and flow rates.
[b]Oscillation observed at some currents and flow rates.
[c]Oscillation never occurred.
[d]Not tested.

power, although this operating condition is not usable because of very high coupling voltage that shorten the neutralizer life time.

Next, a scaling of the fundamental frequency of the coherent wave, ranging over 150–200 kHz was investigated by changing parameters such as $\dot{m}$, d, and l. Table 2 summarizes the frequency of appearance of such oscillations when d and l are changed; it shows that when the ratio of d to l is large, the oscillation is infrequent. We may consider d as a characteristic length describing the diameter of the plasma column blowing out of the neutralizer, and l as a characteristic length describing the plasma column length. Strictly speaking, a plasma column has diameter distribution in the axial direction; increasing l might also increase the column diameter. In that sense, l and d are not perfectly independent parameters.

Although strong oscillations clearly provide a sharp peak, a weak oscillation tends to have a broad spectrum and its representative frequency is not obvious, which causes ambiguity of the peak frequency and is expressed in terms of error bars in the following figures. Figure 12 shows typical variations of oscillation intensities and fundamental frequencies as functions of xenon flow rates. Figure 12a shows that the intensity usually has a peak at certain flow rate and decreases at larger flow rates. Figure 12b illustrates a weak dependence of the frequency on the flow rate and is inclined to decrease as the flow rate increases.

Figure 13 provides the fundamental frequency variations with respect to neutralizer current. The neutralizer current was swept from 100 to 300 mA with an orifice diameter and xenon flow rate, respectively, fixed at 4.5 mm and 0.5 SCCM. The frequency always

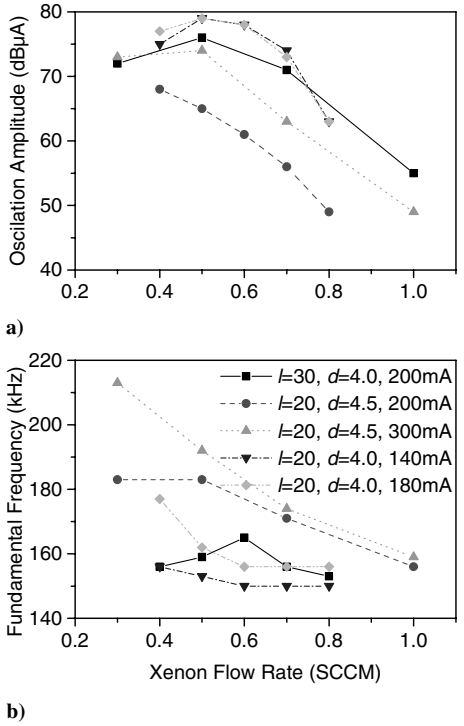

Fig. 12 Typical variation of oscillation intensities and fundamental frequencies as functions of xenon flow rates. $P_\mu = 10$ W.

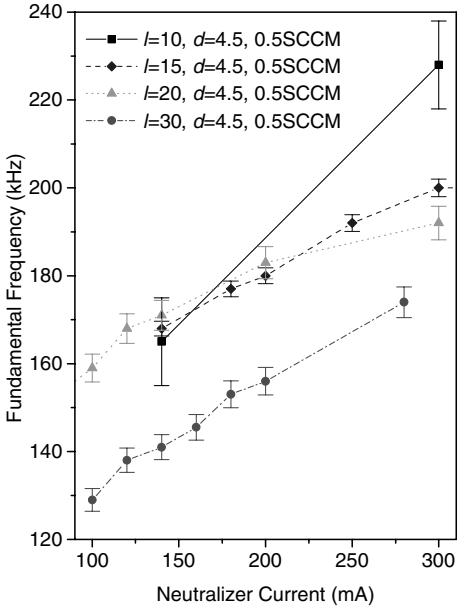

Fig. 13 Fundamental frequency vs neutralizer-current curves weakly dependent on the anode distances l. $d = 4.5$ mm, $\dot{m} = 0.5$ SCCM, $P_\mu = 10$ W.

increases by increasing the current. Four anode distances l were chosen as a parameter. The larger the value of l, the lower the value of the frequency, although such dependence is rather weak.

Figure 14 shows the frequency change as a function of the orifice diameter d. The frequency is smaller when d is larger. In spite of the change of d from 4.0 to 6.0 by a factor of 1.5, the factor by which the accompanied changes lies between 1.3^{-1} and 1.1^{-1}, which can be interpreted as a nearly inversely proportional relation between f and d. With a fixed flow rate, a 1.5 times larger orifice makes the neutral pressure in the neutralizer discharge chamber 2.25 times higher. Because the relationship between the flow rate and the frequency f has a negative slope, as given in Fig. 12, if the pressure is maintained as constant, f and d will tend toward an evident inversely proportional relation.

What is the cause of the coherent noise in the microwave discharge neutralizer at 160 kHz? Oscillations at frequencies lower than the ion plasma frequency are often observed when a current is applied to plasma. Such a phenomenon is generally known as current-driven

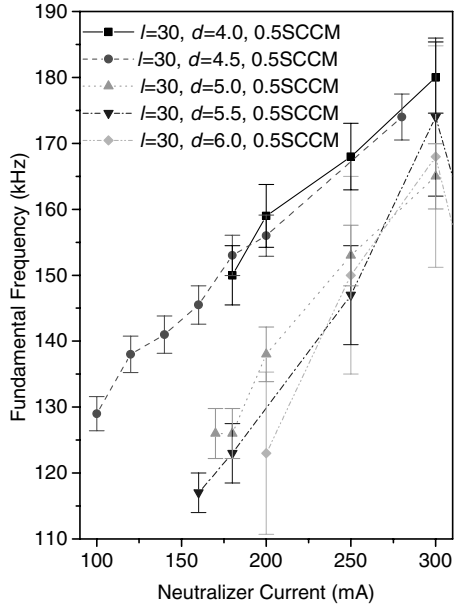

Fig. 14 Fundamental frequency vs neutralizer-current curves dependent on the orifice diameters d. $l = 30$ mm, $\dot{m} = 0.5$ SCCM, $P_\mu = 10$ W.

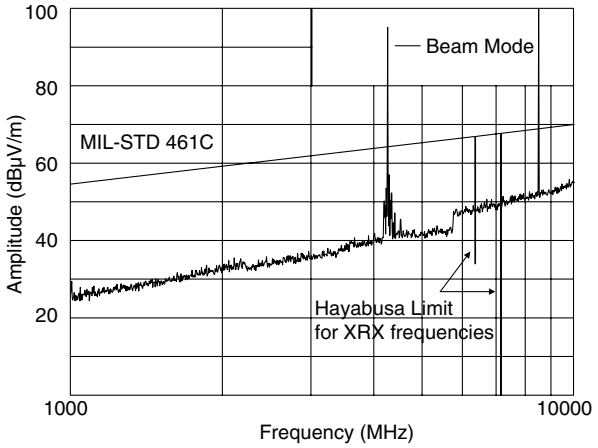

Fig. 15 RE02 narrowband noise (1–10 GHz) from the ion engine system at 7 mN.

ion acoustic instability. Reports have described that, in most cases, it is an oscillation in the axial direction along with the electron current, whose wavelength is twice the plasma column length and whose phase velocity equals the ion sound velocity or the ion thermal velocity [10–12]. Although several interpretations exist for the oscillation mechanism, it is generally thought that the reciprocal of the ion transit time τ_i is calculated using the ion thermal velocity and the plasma column length l:

$$1/\tau_i = \sqrt{3kT_i/m_p}/l \tag{1}$$

That equation fundamentally represents the oscillation frequency, where k is the Boltzmann constant, m_p is the ion mass, and T_i is the ion temperature. Assuming that $T_i = 0.04$ eV, a value of 14 kHz is obtained. However, this value is much smaller than the experimentally observed value of 160 kHz. It is certainly too small to explain oscillation by a longitudinal oscillation mode.

Nevertheless, a report by Crawford [13] offers that the radial mode of an ion acoustic wave is probable. He conducted experiments using several kinds of direct current discharge plasma with hot cathodes and various diameter glass tubes; results revealed low-frequency oscillations below 1 MHz, similar to in our results. According to that publication, the fundamental frequency f is given as

$$f = (2.405/\pi d)(\gamma kT_e/m_p)^{1/2} \tag{2}$$

where d is the diameter, γ is the specific heat ratio (from 1 to 3) and T_e is the electron temperature. The constant 2.405 is the minimum number that makes the Bessel function zero. Assuming that $T_e = 3.5$ eV and $f = 160$ kHz, we obtain $d = 7.7(\gamma = 1)$–$13.2(\gamma = 3)$ mm, which is comparable to the actual orifice size or slightly larger. Radial distribution of neutral-particle density is dependent on the orifice diameter and is a possible constraint of the plasma column diameter in front of the neutralizer. This and the experimentally obtained relation, $fd = $ const., suggest that the radial mode of standing ion acoustic wave exists in the plasma column in front of the microwave discharge neutralizer.

E. RE02 1–10 GHz and X-Band Receiver Interference Test Results

Microwave leakage at frequencies of 4.25 and 8.5 GHz were detected when microwave dummy loads replaced the ion source and the neutralizer in the anechoic chamber. Still, their levels were below the Hayabusa limit by 10 dB and we did not specify the leakage position. The radiated emissions in the discharge mode and beam acceleration mode were too strong to measure with the nominal setup of measuring instruments. As shown in Fig. 15, the obtained data are saturated at the two frequencies. The 4.25 GHz peak has a spread that originates from spurious characteristics of the TWTA and not from nonlinear phenomena of the discharge plasma. These emissions at two frequencies are caused by leakage of the supplied microwave power through the grid holes of the ion beam optics and the neutralizer orifice.

The radiated emissions, which were measured again without the normally used preamplifier and a 20 dB attenuator, are summarized in Table 3. The microwave leakage was 10 dB larger in the beam acceleration than in the plasma discharge at the electron cyclotron resonance frequency of 4.25 GHz. The plasma density inside the ion source is close to the so-called cutoff density (2.2×10^{17} m^{-3}@4.25 GHz); microwaves of 4.25 GHz or lower frequencies cannot travel through the plasma easily. In beam mode the density is smaller than in discharge mode. The leakage increases because the plasma density inside the ion source is lower in beam mode than in discharge mode. For emission at the second harmonic frequency of 8.5 GHz, the leakage is independent of the plasma density. There is originally no absorption by the plasma at that frequency. In this experiment using the cylindrical glass chamber, the thrust level was throttled to 80% by reducing mass flow rate and maintaining microwave power, but it turned out to be a more severe testing condition from the viewpoint of microwave noise emission, in which the plasma density was lower and noise leakage increased. The leaked powers are calculable as 66 mW at 4.25 GHz and 1.9 mW at 8.50 GHz if we assume that the leaked electromagnetic wave from the IES is an isotropic wave. For effective use of supplied microwave power of about 40 W for plasma generation in an ion source and a neutralizer, these losses are sufficiently small and are not problematic.

To provide a reference to reflect the radiated susceptibility (RS) specification of Hayabusa, E-field intensities at a distance of 1 m were calculated as shown in Table 3. In the original Hayabusa specification the required level was determined as 5 V · m^{-1} for high frequencies over 30 MHz. As an illustrative example, assuming the worst case in which equipment is located at a distance of r from thruster heads and N ion engines are operated simultaneously, the E-field intensity E at that position would be calculated as

$$E = N \times E_{\mathrm{RE02}} \sqrt{(1/r)^2} \tag{3}$$

assuming isotropic and far-field $1/r^2$ power fall-off and coherent (E-fields add) combination of the thruster emissions at the field point. Given $N = 3$, $E_{\mathrm{RE02}} = 3.3$ V · m^{-1}, $r = 0.5$ m yield E = 19.8 V · m^{-1}.

Therefore, the RS specification at 4.2 GHz was modified to 20 V · m^{-1} and the RE specification was waived for the IES. The philosophy of the RS specification at the RF frequency for plasma production of microwave discharge ion thrusters might be identical to those of other transmitters onboard the spacecraft.

The power density at the 7.16 GHz X-band uplink frequency was calculated from results of the interference test with the PM of the XRX. Table 4 shows the change of the noise level detected by the XRX depending on the operating condition of the IES. Because more noise was observed when no plasma existed or its density was smaller, it is thought that very weak spurious signals originating at the microwave amplifier leaked from the ion source as well as from the neutralizer at 7.16 GHz. The low-gain antenna C (LGA-C) of the Hayabusa spacecraft, which is closest to the IES and is affected easily by radiated emissions when used as receiving antenna of the XRX, is

Table 3 Microwave leakage at 1 m at oscillator frequency, its second harmonic, and X-band uplink frequency of Hayabusa spacecraft

	4.25 GHz	8.5 GHz	7.16 GHz
Operating at 7 mN	130.4 dB μV · m^{-1} (3.3 V/m)	99.7 dB μV · m^{-1} (0.097 V/m)	−48.72 dB μV · m^{-1}
Main and neutralizer discharge	119 dB μV · m^{-1} (0.89 V/m^{-1})	99.2 dB μV · m^{-1} (0.091 V/m^{-1})	−48.82 dB μV · m^{-1}

Table 4 Noise levels observed with the X-band receiver at several IES conditions

Ion source	Neutralizer	Noise level relative to XRX internal noise level
Beam extraction	Electron extraction	0.6 dB
Discharge	Discharge	0.5 dB
Discharge	Microwave introduction without Xe gas	0.7 dB
Microwave introduction without Xe gas	Microwave introduction without Xe gas	1.1 dB
No operation	No operation	0 dB (background noise floor)

calculated to couple to the XRX receiver an estimated IES noise power of -210.2 dB m $\cdot$ Hz^{-1} considering the distance, the angle separation and the antenna gain pattern. This noise power is sufficiently small compared to the internal noise level (-173 dB m $\cdot$ Hz^{-1}) of the receiving system. Therefore, we infer that no adverse effect is given to the XRX, even in the case when the three ion engines are operating at the same time with maximal thrust levels.

IV. Conclusions

Comparing the results of EMI measurements using the IES of the Hayabusa asteroid sample return mission and the neutralizer operating independently, it was found that radiated emissions from the IES exceeding the MIL-STD-461C originate mainly from the neutralizer. Radiated emission in the high-frequency range above 1 GHz was not observed, except at the oscillator and second harmonic frequency of the TWTA used for plasma production, which leaks from the exit of both the ion source and the neutralizer. It is concluded that the operation of the IES does not interfere with the XRX of the Hayabusa, based on findings of the test using the PM of the XRX. Although the IES was granted a waiver on RE specifications, the final check for electromagnetic compatibility between the IES and the spacecraft was carried out using the ion engine operation in a glass chamber located in the vicinity of the flight model of the Hayabusa spacecraft in a clean room and by three ion engines operating during thermal vacuum tests in which the IES was fully integrated into the spacecraft.

Acknowledgments

The authors wish to thank Z. Yamamoto and Y. Kamata of the Institute of Space and Astronautical Science/Japan Aerospace Exploration Agency (ISAS/JAXA), F. Fuke of the Nippon Electronics Company (NEC), and the rest of the Hayabusa communication subsystem staff for their cooperation in this series of tests.

References

[1] Sovey, J. S., Carney, L. M., and Knowles, S. C., "Electromagnetic Emission Experiences Using Electric Propulsion Systems," *Journal of Propulsion and Power*, Vol. 5, No. 5, 1989, pp. 534–547.

[2] Nakamura, Y., and Kitamura, S., "Research on 5 cm Diameter Mercury Ion Thruster," *Acta Astronautica*, Vol. 7, Nos. 8–9, Aug.–Sept. 1980, pp. 1075–1089.

[3] Kudo, I., Machida, K., Toda, Y., and Murakami, H., "Electromagnetic Noise from an Ion Engine System," *Journal of Spacecraft and Rockets*, Vol. 20, No. 1, 1983, pp. 84–88.

[4] Shimada, S., Takegahara, H., Gotoh, Y., Satoh, K., and Kajiwara, K., "Ion Engine System Development of ETS-VI," AIAA Paper 89-2267, 1989.

[5] Muller, H., Kukies, R., and Bassner, H., "EMC Tests on the RITA Ion Propulsion Assembly for the ARTEMIS Satellite," AIAA Paper 92-3208, 1992.

[6] Chanda, S., Mawdsley, F., Brown, R. D., Watson, S. D., Malik, A. K., and Fearn, D. G., "Measurements of the Electromagnetic Emissions from the T5 Ion Thruster," International Electric Propulsion Conference Paper 93-234, 1993.

[7] Wang, J., Brinza, D. E., Young, D. T., Nordholt, J. E., Polk, J. E., Henry, M. D., Goldstein, R., Hanley, J. J., Lawrence, D. J., and Shappirio, M., "Deep Space One Investigations of Ion Propulsion Plasma Environment," *Journal of Spacecraft and Rockets*, Vol. 37, No. 5, 2000, pp. 545–555.

[8] Kuninaka, H., Shimizu, Y., Yamada, T., Funaki, I., and Nishiyama, K., "Flight Report During Two Years on HAYABUSA Explorer Propelled by Microwave Discharge Ion Engines," AIAA Paper 2005-3673, 2005.

[9] Onodera, N., Takegahara, H., Funaki, I., and Kuninaka, H., "Interaction Between Plasma Plume of Electric Propulsion and Spacecraft Communication," International Electric Propulsion Conference Paper 99-228, 1999.

[10] Alexeff, I., and Neidigh, R. V., "Observations of Ionic Sound Waves in Plasmas Their Properties and Applications," *Physical Review*, Vol. 129, No. 2, Jan. 1963, pp. 516–527.

[11] Barkan, A., D'Angelo, N., and Merlino, R. L., "Potential Relaxation Instability and Ion Acoustic Waves in a Single-Ended Q-Machine Dusty Plasma," *Physics Letters A*, Vol. 222, No. 5, Nov. 1996, pp. 329–332.

[12] Capeau, C. A., Bachet, G., and Doveil, F., "Plasma Self-Oscillations in the Temperature-Limited Current Regime of a Hot Cathode Discharge," *Physics of Plasmas*, Vol. 2, No. 12, Dec. 1995, pp. 4650–4655.

[13] Crawford, F. W., "Electrostatic Sound Wave Modes in a Plasma," *Physical Review Letters*, Vol. 6, No. 12, June 1961, pp. 663–665.

A. Gallimore
Associate Editor